Journal of Visualized Experiments

Ultrasound Imaging of the Thoracic and Abdominal Aorta in Mice to Determine Aneurysm Dimensions

--Manuscript Draft--

Article Type:	Invited Methods Article - JoVE Produced Video
Manuscript Number:	JoVE59013R2
Full Title:	Ultrasound Imaging of the Thoracic and Abdominal Aorta in Mice to Determine Aneurysm Dimensions
Keywords:	ultrasound imaging; aortic dimension; aortic aneurysm; aorta; aortic sinus; ascending aorta; abdominal aorta
Corresponding Author:	Hong Lu UNITED STATES
Corresponding Author's Institution:	
Corresponding Author E-Mail:	hlu4@uky.edu
Order of Authors:	Hisashi Sawada
	Jeff Z. Chen
	Bradley C. Wright
	Jessica J. Moorleghen
	Hong Lu
	Alan Daugherty
Additional Information:	
Question	**Response**
Please indicate whether this article will be Standard Access or Open Access.	Open Access (US$4,200)
Please indicate the **city, state/province, and country** where this article will be **filmed**. Please do not use abbreviations.	Lexington, Kentucky, United States

TITLE:

Ultrasound Imaging of the Thoracic and Abdominal Aorta in Mice to Determine Aneurysm Dimensions

AUTHORS & AFFILIATIONS:

Hisashi Sawada[1], Jeff Z. Chen[2], Bradley C. Wright[1], Jessica J. Moorleghen[1], Hong S. Lu[1,2], Alan Daugherty[1,2]

[1]Saha Cardiovascular Research Center, University of Kentucky, Lexington, KY, USA

[2]Department of Physiology, University of Kentucky, Lexington, KY, USA

Corresponding Author:

Alan Daugherty (alan.daugherty@uky.edu)

E-mail Addresses of Co-authors:

Hisashi Sawada (hisashi.sawada@uky.edu)

Jeff Z. Chen (jeff.chen@uky.edu)

Bradley C. Wright (bradley.wright@uky.edu)

Jessica J. Moorleghen (jjmoorl@uky.edu)

Hong S. Lu (hong.lu@uky.edu)

KEYWORDS:

Ultrasound imaging, aortic dimensions, aorta, aortic sinus, ascending aorta, abdominal aorta, aortic aneurysm

SUMMARY:

Ultrasound imaging has become a common modality to determine the luminal dimensions of thoracic and abdominal aortic aneurysms in mice. This protocol describes the procedure to acquire reliable and reproducible two-dimensional ultrasound images of the ascending and abdominal aorta in mice.

ABSTRACT:

Contemporary high-resolution ultrasound instruments have sufficient resolution to facilitate the measurement of mouse aortas. These instruments have been widely used to measure aortic dimensions in mouse models of aortic aneurysms. Aortic aneurysms are defined as permanent dilations of the aorta, which occur most frequently in the ascending and abdominal regions. Sequential measurements of aortic dimensions by ultrasound are the principal approach for assessing the development and progression of aortic aneurysms in vivo. Although many reported studies used ultrasound imaging to measure aortic diameters as a primary endpoint, there are confounding factors, such as probe position and cardiac cycle, that may impact the accuracy of data acquisition, analysis, and interpretation. The purpose of this protocol is to provide a practical guide on the use of ultrasound to measure the aortic diameter in a reliable and reproducible manner. This protocol introduces the preparation of mice and instruments, the acquisition of appropriate ultrasound images, and data analysis.

INTRODUCTION:

Aortic aneurysms are common vascular diseases characterized by a permanent luminal dilation of the thoracic and/or abdominal aorta[1–4]. No pharmacological therapies have been established to prevent the dilation and rupture of aortic aneurysms, which emphasizes the need for insights into pathogenic mechanisms. To elucidate the mechanisms of aortic aneurysms, mouse models produced by genetic or chemical manipulations have been widely used[4–12]. The accurate quantification of the aortic diameter in mice is the basis of aortic aneurysm research.

The development of high-frequency ultrasound has increased the spatial and temporal resolution of images to detect small differences in aortic dimensions[13–15]. This has enabled the sequential measurement of aortic diameters in mice, and thus, it has become the preferred method for measuring aortic diameters in murine studies of aortic aneurysms. Although ultrasound imaging is a simple technique, knowledge of aortic anatomy and physiology is required to acquire appropriate images for accurate measurements, data analysis, and interpretation. The aorta is a pulsating cylindrical organ with variable curvatures in the proximal thoracic region[16]. This contributes to the potential for an inaccurate determination of aortic dimensions in the commonly acquired two-dimensional (2D) images. The accuracy of aortic measurements could be compromised further by aortic tortuosity in aneurysmal state[17]. To obtain reliable and reproducible measurements of aortic dilations, this protocol provides a practical guide for the use of a high-resolution ultrasound system to measure proximal thoracic and abdominal aortic diameters in mice.

PROTOCOL:

Ultrasound imaging in mice is performed with approval of the University of Kentucky Institutional Animal Care and Use Committee (IACUC protocol number: 2018-2967). During the imaging, the mice are anesthetized using isoflurane 1%–3% vol/vol and placed on a heating platform to reduce procedural stress and prevent hypothermia. Eye lubricant is applied to prevent corneal damage due to the loss of the blink reflex during anesthesia.

1. Equipment setup

1.1. Turn on the ultrasound machine, heating platform, and gel warmer (**Figure 1**).

1.2. Open the ultrasound program. Enter the study information, such as the study name and mouse information.

1.3. Check the isoflurane vaporizer and O_2 tank. If the content is low, fill the isoflurane vaporizer and/or exchange it for a new O_2 tank.

1.4. Connect the anesthetic scavenging filters to the induction chamber and the nose cone.

1.5. Open the branch for the induction chamber.

1.6. Turn on the O_2 tank.

1.7. Turn the O_2 and isoflurane knobs on the anesthesia vaporizer to 1 L/min and 0% vol/vol, respectively, to fill the chamber with O_2.

2. Preparation of the mouse

2.1. Place the mouse in the O_2-filled induction chamber to minimize unwanted cardiovascular changes due to anesthesia.

2.2. Turn on the isoflurane vaporizer (1.5%–2.5 % vol/vol).

2.3. Confirm the absence of the hind limb withdrawal reflex.

2.4. Remove the mouse from the chamber and place one drop of sterile ophthalmic lubricant in each eye.

2.5. Redirect the anesthesia to the nose cone and close the flow to the induction chamber.

2.6. Lay the mouse dorsally on the heating platform with its nose in the anesthesia nose cone.

2.7. Apply depilatory cream to the chest or abdomen, using a cotton swab. Minimize the amount of depilatory cream use to avoid irritation.

2.8. Wait for 1 min, and then, gently wipe off all cream and hair.

2.9. Irrigate the area with warm water and wipe it dry to completely remove the cream.

2.10. Dot gel on each of the four copper leads on the platform.

2.11. Tape each paw pad down (palms down) to the leads for electrocardiogram (ECG) readings. This will provide the ECG and respiratory physiology of the mouse while anesthetized.

2.12. Verify that the heart rate is between 450–550 beats/min. Since anesthesia affects cardiac function, which can alter the aortic diameter, adjust the delivery rate of anesthesia so that the heart rate is in an appropriate range.

2.13. Apply prewarmed ultrasonic gel to the prepared site.

2.14. Attach the probe to the holder.

2.15. Rotate the platform for optimal scanning and lower the probe until it is in contact with the ultrasonic gel.

3. Imaging of the thoracic aorta

3.1. Tilt down the platform to the left side of the mouse.

3.2. Put the probe on the right edge of the mouse's sternum (**Figure 2A**). Orient the reference marker on the probe caudally.

NOTE: The reference marker on the probe indicates the probe direction and is consistent with the maker on the monitor of the ultrasound system (**Figure 2A–D**). The shape of the marker varies in each ultrasound system.

3.3. Use color Doppler on the thoracic aorta to confirm blood flow.

3.4. Adjust the stage and probe angle to show the aorta clearly (**Figure 3A,B**).

NOTE: The aortic valve and innominate and pulmonary arteries can be used for anatomical landmarks for the right parasternal long axis view. Therefore, aortic images from this view can include the aortic valve and innominate and pulmonary arteries in one frame (**Figure 3A**). If it is difficult to capture the entire ascending aorta in one scan, due to aortic pathologies such as aortic dilation and tortuosity, the images should be captured separately. Since separated images have the potential to cause an underestimation of the aortic measurements, fine positioning of the stage and probe is required. The right parasternal long axis view is optimal for imaging the entire ascending aorta (**Figure 3C**). However, it is often difficult to capture the aortic sinus in this view, especially in aneurysmal aortas. The left parasternal long axis view enables a capture from the aortic root to the proximal ascending aorta as an alternative approach, although this view cannot capture the aortic arch in one frame (**Figure 3C**). For the left parasternal long axis view, put the probe on the left edge of the sternum (**Figure 2B**). The stage is flat or slightly tilted to the mouse's right. Carry out the other steps of the procedure in the same manner as the right parasternal long axis view. Advantages and disadvantages of these probe positions are described in **Table 2**. Aortic images must be captured consistently in either right or left parasternal long axis view.

3.5. Crop the ultrasound image to increase the frame rate, using the knobs for image depth and width.

3.6. Change the focal depth on the dorsal side of the ascending aorta, using the knob for focal depth.

3.7. Verify the ultrasound parameters. The ultrasound settings for this protocol are described in **Table 1**.

3.8. Move the probe gently, using the X- and Y-axis stage knob, to capture the longitudinal aortic image with the largest possible diameter.

3.9. Store one cine loop.

4. Imaging of the abdominal aorta

4.1. Place the probe transversely, just below the sternum and xiphoid process (**Figure 2C**). The reference marker on the probe should face the mouse's right side. The abdominal aorta should be located next to the inferior vena cava and/or portal vein (**Figure 3D**).

4.2. Visualize the abdominal aorta with color Doppler to confirm pulsatile flow.

NOTE: If the Doppler angle is perpendicular to the blood flow, a color Doppler signal will not appear in the aorta. In addition to color Doppler imaging, the abdominal aorta can be distinguished from the vena cava and portal vein by slightly pressing down the probe. The vena cava and portal vein are compressible, while the aorta maintains its patency.

4.3. Crop the ultrasound image to increase the frame rate.

4.4. Change the focal depth to the posterior wall of the abdominal aorta.

4.5. Move the probe caudally to visualize the branch points of the celiac and superior mesenteric arteries.

4.6. Locate the right renal artery and use it as a landmark.

NOTE: Since abdominal aortic aneurysms may lead to aortic tortuosity, adjust the probe angle to image the abdominal aorta perpendicularly. For an internal control, one image of the right renal branch point should be captured.

4.7. Capture a cine loop of the region of interest which shows the maximum dilation in the abdominal aorta (**Figure 3D,E**).

NOTE: The localization of aortic aneurysms varies in each animal model. Aortic dilation in angiotensin II-induced mice occurs predominantly in the suprarenal aorta, while $CaCl_2$ or elastase induces aortic aneurysm in the infrarenal aortic in mice.

5. Postscanning mouse care and cleanup

5.1. Wipe off the ultrasonic gel, irrigate the chest or abdomen with warm water, and gently wipe the mouse dry.

5.2. Return the mouse to its cage, which is placed on a heating pad.

5.3. Turn off the isoflurane vaporizer and O_2 tank. Refill the vaporizer if the isoflurane level is low.

5.4. Clean the ultrasound machine, probe, and platform with a soft cloth and isopropyl alcohol or glutaraldehyde wipes.

5.5. Download all files collected during the scan.

5.6. Turn off the ultrasound machine.

5.7. Return the mice to animal housing rooms after they have recovered from the anesthesia.

6. Analysis

6.1. Analysis of thoracic aortic images

6.1.1. Launch the analysis software and open the ultrasound data. An example image of analysis software (Vevo LAB 3.0.0) is shown in **Supplemental Figure 1**.

6.1.2. Select one aortic ultrasound image for measurements from the cine loop (**Figure 4A,C,E,G** and **Supplemental Figure 1**).

NOTE: This protocol typically detects six to seven heartbeats in one cine loop. Since the aortic diameter is different between systole and diastole (**Figure 4A–G**), the measurements need to be examined at a consistent phase of the cardiac cycle. Systole is defined from the R wave to the end of the T wave. In general, T waves are difficult to identify in mouse ECG. Therefore, the aortic diameter in systole should be measured at physiologic systole, defined by visual inspection (**Figure 4I**). The cardiac phase when the aorta is maximally expanded should be midsystole. End-diastole is easily defined at the R wave of the ECG (**Figure 4I**). Aortic measurements in end-diastole are simpler than those in midsystole in terms of distinguishing the cardiac cycle.

6.1.3. Draw a line in the center of the aortic lumen. This center line will be used to ensure that the measurement lines are perpendicular to the aorta (**Figure 4B,D** and **Supplemental Figure 1**).

6.1.4. Draw perpendicular lines through the center line from the luminal inner edge to inner edge at the aortic sinus and maximal ascending aortic levels (**Figure 4B,D** and **Supplemental Figure 1**).

6.1.5. Measure the aortic diameter in at least three separate heartbeats and calculate the mean of the measurements.

NOTE: The Vevo2100 system uses the Vevo LAB analysis software for measurements of aortic dimension. Brief explanations for each button are as follows. Measurement mode (**Supplemental Figure 1A**): this mode must be selected for aortic measurements. The slider of a cine loop (**Supplemental Figure 1B**): the ultrasound frame is selected using this slider. Traced distance (**Supplemental Figure 1C**): the center line is drawn with this function. Linear distance (**Supplemental Figure 1D**): the aortic dimension is measured using this function.

6.2. Analysis of abdominal aortic images

6.2.1. Launch the analysis software and open the ultrasound data.

6.2.2. Select an aortic image for analysis from the cine loop (**Figure 4E,G**).

NOTE: Similar to thoracic aortic measurements, the cardiac cycle may affect the abdominal aortic diameter and area. Measurements should be determined at a consistent phase of the cardiac cycle.

6.2.3. Draw a line across the largest luminal diameter, from the inner edge to the inner edge of the vessel lumen (**Figure 4F,H**).

6.2.4. Trace the inner edge of the aortic lumen for the luminal area (**Figure 4F,H**).

6.2.5. Acquire aortic measurements at a minimum of three separate heartbeats and calculate the mean of the data.

REPRESENTATIVE RESULTS:

Representative ultrasound images of nonaneurysmal proximal thoracic and abdominal aorta are shown in **Figure 3A** and **Figure 3C**, respectively. The ascending aorta is located next to the pulmonary artery and forms a curved tube with three branches in the arch region: the innominate artery, the left common carotid artery, and the left subclavian artery (**Figure 3A**). The abdominal aorta is detected dorsally to the inferior vena cava (**Figure 3D**). Representative images of thoracic and abdominal aortic aneurysms with profound dilations, as compared with normal diameters in **Figure 3A** and **Figure 3D**, are shown in **Figure 3B** and **Figure 3H**, respectively. All ultrasound images were captured at end-diastole.

Representative thoracic and abdominal aortic ultrasound images were captured at the midsystole and end-diastole (**Figure 4A,C,E,G**). Representative images showing measurements are presented in **Figure 4B,D,F,H**. The green line in the center of the ascending aorta was used for standardizing the aortic sinus and ascending aortic diameter (**Figure 4B,D**). Lines were drawn perpendicularly to the green line between the two inner edges of the lumen at the aortic sinus (yellow line) and the maximal ascending aortic diameter (red line). The luminal diameters of the thoracic and abdominal aortas were different between systole and diastole (**Figure 4A–H**). For the abdominal aorta, the maximal aortic diameter (red) and luminal area (green) were measured (**Figure 4F,H**). A representative image of the monitor electrocardiogram is shown in **Figure 4I**. The cardiac cycle needs to be considered for accurate measurements. The end-diastole and systole are indicated by the white dotted and pink lines, respectively.

To validate the accuracy and reproducibility of this protocol, we performed a pilot study. Representative thoracic aortic ultrasound and ex vivo images are shown in **Figure 5A**. There was no major difference in diameters measured between these images for the ascending aortic diameter (ultrasound: 1.67 mm vs. ex vivo: 1.65 mm). Since the aortic sinus was difficult to see in the ex vivo image, the aortic sinus diameter was not measured ex vivo. The inter- and intraobserver reproducibility of this protocol are shown in **Figure 5B,C**. To determine potential

variabilities, ultrasound imaging was performed by two observers independently, namely by an experienced cardiologist and a nonexperienced undergraduate student who is learning this technique, on two different days, using the same mice (*n* = 5). All dots were located between the mean ± 1.96 SD in **Figure 5B,C**, which indicates no major inter- or intraobserver variabilities for this protocol.

FIGURE LEGENDS:

Figure 1: Workstation setup. The workstation includes the induction chamber for anesthesia, anesthetic scavenging filters, the heated platform, the ultrasound gel, and the gel warmer.

Figure 2: Examples of probe placement for proximal thoracic and abdominal aortic imaging. Probe placement for (**A**) the right and (**B**) **the** left parasternal long axis view of the aortic root, ascending and arch regions, and (**C**) the short axis view of the abdominal aorta. (**D**) A representative monitor image of the ultrasound system. The black arrows indicate the reference marker on the probe. The yellow arrow indicates the side of the reference marker.

Figure 3: Representative ultrasound images of the thoracic and abdominal aorta. (**A**) Nonaneurysmal and (**B**) aneurysmal ascending aorta, from the right parasternal long axis view. (**C**) Nonaneurysmal ascending aorta, from the left parasternal long axis view. (**D**) Nonaneurysmal and (**E**) aneurysmal abdominal aorta. Asc Ao = ascending aorta, IA = innominate artery, LCA = left common carotid artery, LSA = left subclavian artery, PA = pulmonary artery, Sinus = aortic sinus, IVC = inferior vena cava, and Abd Ao = abdominal aorta. The yellow triangles indicate an aortic aneurysm.

Figure 4: Measurements of aortic images. Images of the thoracic aorta captured at (**A**) the midsystole and (**C**) the end-diastole. Images showing measurements of aortic diameters in the proximal thoracic aortic region during (**B**) midsystole and (**D**) diastole. The green line indicates the center of the ascending aorta. The yellow and red lines indicate diameters of the aortic sinus and ascending aorta, respectively. Digits in yellow and red colors indicate actual diameters of the aortic sinus and ascending aorta, respectively. Images of abdominal aorta captured at (**E**) the midsystole and (**G**) the end-diastole. Images showing measurements of the suprarenal aorta during (**F**) midsystole and (**H**) end-diastole. The red and green lines indicate the diameter and luminal area of the abdominal aorta, respectively. Digits in red and green colors indicate the actual diameter and are of the abdominal aorta, respectively. (**I**) Monitor electrocardiogram (ECG) recorded during the image acquisitions. The green and yellow lines indicate the ECG and respiratory cycle, respectively. The white dotted line indicates the end-diastole, and the purple line indicates systole. P = P wave and R = R wave.

Figure 5: Accuracy and reproducibility of ultrasound imaging. (**A**) Representative images of thoracic aortic ultrasound and ex vivo images in C57BL/6J male mice (10–12 weeks old). Bland–Altman plots show (**B**) inter- and (**C**) intraobserver variabilities of this protocol. Asc Ao = ascending aorta, IA = innominate artery, LCA = left common carotid artery, LSA = left subclavian artery, PA = pulmonary artery, and Sinus = aortic sinus. The green line indicates the center of the ascending

aorta. The yellow and red lines indicate the diameters of the aortic sinus and ascending aorta, respectively. Digits in red colors denote the actual diameters of the ascending aorta measured in ultrasound and ex vivo images. The black dotted lines indicate the mean and mean ± 1.96 SD.

Supplemental Figure 1: Example image of ultrasound analysis software. Ultrasound data analysis must be performed in (**A**) measurement mode. One aortic ultrasound image is selected for analysis from the cine loop using (**B**) the slider of a cine loop. The center line is drawn using (**C**) the traced distance function. The aortic dimension is measured by (**D**) the linear distance function.

DISCUSSION:

This protocol provides a technical guide for the image acquisition of the thoracic and abdominal aorta in mice, using a high-frequency ultrasound system. Ultrasound aortic imaging has potential confounders, such as probe position and cardiac cycle, that may compromise the accuracy of the aortic measurements, particularly in the proximal thoracic aorta. This protocol describes detailed instructions and strategies for image acquisition, measurement, and data analysis, in order to accurately measure aortic dimensions.

For imaging the proximal thoracic aorta, there are several approaches to probe placement. The right parasternal long axis view shown in **Figure 2A** was used for ultrasound imaging in this protocol. This view facilitates the acquisition of high-quality images from the aortic sinus to the aortic arch portion. It is not optimal for the descending aorta because of interference of the ultrasonic waves. This protocol is applicable to most mouse models of thoracic aortic aneurysms because they exhibit luminal dilation predominantly in the aortic root to the ascending aorta. This includes chronic angiotensin II infusion that causes aneurysm formation in the ascending aorta of mice[18–23]. Mouse models of Marfan syndrome (fibrillin $1^{C1041G/+}$ and fibrillin $1^{mgR/mgR}$ mice) display both aortic root and ascending aortic dilation[23–25]. Loeys-Dietz syndrome mouse models (postnatal deletion of TGF-β receptor 1 or 2 in smooth muscle cells) also develop aneurysm in the aortic root and ascending aorta[18,26–28]. Therefore, the right parasternal long axis view is appropriate for aortic imaging in these mouse models of thoracic aortic aneurysms. On the other hand, the right parasternal short axis view has the potential to capture aortic images diagonally because aneurysms are often complicated by aortic tortuosity, which may cause an overestimation of diameters. Unlike the thoracic aorta, the short axis view was used for the imaging of the abdominal aorta in this protocol. Since aortic curvature and tortuosity are modest in the abdominal aorta compared to the thoracic aorta, the acquisition of images in the short axis view ameliorates underestimations of the aortic diameter. It is important to note that different probe positions provide different viewing angles, and the aortic diameter may be different in each view angle. Therefore, reliable aortic diameter measurements are enhanced by applying the same probe position for all images within a study. Interestingly, three-dimensional (3D) ultrasound images of the heart and aorta have been reported recently[29–32]. In addition, current ultrasound systems can obtain 3D images over time as four-dimensional images[33]. Thus, these 3D imaging technologies have the potential to demonstrate the aortic structure more precisely, which may solve the problem of probe positioning.

Ultrasound images can be captured in either 2D brightness mode (B-mode) or one-dimensional motion mode (M-mode). Although some articles have used M-mode for the measurement of aortic diameter, B-mode is preferable[15,34–36]. M-mode has the capacity to image in two dimensions to increase temporal and spatial resolution. However, this mode relies on the assumption that the aorta is a concentric cylinder being imaged perpendicularly to the ultrasonic waves. This assumption may not hold true in an aneurysmal state and the curvature of the ascending aorta makes this difficult, even in nonaneurysmal states. In addition, the aorta does not remain in a fixed position throughout the cardiac cycle[37]. Therefore, M-mode may cause measurement errors, including over- and underestimations.

It is also important to note that the cardiac cycle affects the luminal diameter in the aorta. As expected, the aortic diameter in systole is greater than in diastole (**Figure 4A–H**), which is associated with aortic wall elasticity and strain. Aortic wall elasticity and strain can be calculated from the difference of aortic diameters between systole and diastole. Elasticity and strain are decreased in aneurysmal aortas compared to normal aortas[31,34,35,38–40]. Aortic stiffness cannot be measured directly by ultrasound. Measuring pulse wave velocity (PWV) can evaluate its stiffness as a proxy, which is reported to be increased in aneurysmal aortas[31,35,41,42]. PWV is calculated by the transit time between two arterial sites, using pulse wave Doppler images and their corresponding distance. For comparing aortic diameters, unlike clinical examination, there is no rigorous standardization in terms of cardiac phase for aortic measurements in mice. Therefore, it is still unclear which cardiac phase is appropriate for aortic measurements. However, to ensure reliable and reproducible comparisons, aortic diameters should be measured in a defined phase of the cardiac cycle.

This protocol provides detailed instructions for aortic imaging and data analysis in order to measure aortic dimensions accurately. The aortic measurement, using this protocol, was consistent with the actual ex vivo aortic diameter (**Figure 5A**). We also confirmed consistencies of inter- and intraobserver reproducibility (**Figure 5B,C**). All steps in this protocol, especially probe position and cardiac cycle, are necessary for accurate measurements. However, even when using appropriate procedures, artifacts during ultrasound imaging are unavoidable. The location of ribs and lung, as well as respiration and cardiac pulsation, can affect the image quality of the thoracic aorta. Intestinal gas can also cause artifacts in abdominal imaging. Thus, we suggest defining exclusion criteria when following this protocol in case of poor aortic images.

With the advent of high-resolution ultrasound systems, the aortic structure of mice can be examined in exquisite detail, both serially and conventionally, thereby greatly contributing to the understanding of aortic aneurysms. Ultrasound imaging, with the protocol as described above, is a reliable and reproducible noninvasive approach for quantifying aortic aneurysms in mice.

ACKNOWLEDGMENTS:
The authors' research work was supported by the National Heart, Lung, and Blood Institute of the National Institutes of Health under award numbers R01HL133723 and R01HL139748 and the American Heart Association SFRN in Vascular Disease (18SFRN33960001). H.S. is supported by an AHA postdoctoral fellowship (18POST33990468). J.C. is supported by NCATS UL1TR001998. The

content in this manuscript is solely the responsibility of the authors and does not necessarily represent the official views of the National Institutes of Health.

DISCLOSURES:

The authors have nothing to disclosure.

REFERENCES:

1. Hiratzka, L. F. et al. 2010 ACCF/AHA/AATS/ACR/ASA/SCA/SCAI/SIR/STS/SVM guidelines for the diagnosis and management of patients with Thoracic Aortic Disease: a report of the American College of Cardiology Foundation/American Heart Association Task Force on Practice Guidelines, American Association for Thoracic Surgery, American College of Radiology, American Stroke Association, Society of Cardiovascular Anesthesiologists, Society for Cardiovascular Angiography and Interventions, Society of Interventional Radiology, Society of Thoracic Surgeons, and Society for Vascular Medicine. *Circulation.* **121** (13), e266-369 (2010).
2. Robinet, P. et al. Consideration of Sex Differences in Design and Reporting of Experimental Arterial Pathology Studies-Statement From ATVB Council. *Arteriosclerosis, Thrombosis, and Vascular Biology.* **38** (2), 292-303 (2018).
3. Wanhainen, A., Mani, K., Golledge, J. Surrogate Markers of Abdominal Aortic Aneurysm Progression. *Arteriosclerosis, Thrombosis, and Vascular Biology.* **36** (2), 236-244 (2016).
4. Lu, H., Daugherty, A. Aortic Aneurysms. *Arteriosclerosis, Thrombosis, and Vascular Biology.* **37** (6), e59-e65 (2017).
5. Angelov, S. N., Zhu, J., Dichek, D. A. New Mouse Model of Abdominal Aortic Aneurysm: Put Out to Expand. *Arteriosclerosis, Thrombosis, and Vascular Biology.* **37** (11), 1990-1993 (2017).
6. Daugherty, A., Manning, M. W., Cassis, L. A. Angiotensin II promotes atherosclerotic lesions and aneurysms in apolipoprotein E-deficient mice. *The Journal of Clinical Investigation.* **105** (11), 1605-1612 (2000).
7. Kanematsu, Y. et al. Pharmacologically induced thoracic and abdominal aortic aneurysms in mice. *Hypertension.* **55** (5), 1267-1274 (2010).
8. Longo, G. M. et al. Matrix metalloproteinases 2 and 9 work in concert to produce aortic aneurysms. *The Journal of Clinical Investigation.* **110** (5), 625-632 (2002).
9. Pyo, R. et al. Targeted gene disruption of matrix metalloproteinase-9 (gelatinase B) suppresses development of experimental abdominal aortic aneurysms. *The Journal of Clinical Investigation.* **105** (11), 1641-1649 (2000).
10. Raffort, J. et al. Monocytes and macrophages in abdominal aortic aneurysm. *Nature Reviews Cardiology.* **14** (8), 457-471 (2017).
11. Senemaud, J. et al. Translational Relevance and Recent Advances of Animal Models of Abdominal Aortic Aneurysm. *Arteriosclerosis, Thrombosis, and Vascular Biology.* **37** (3), 401-410 (2017).
12. Wilson, N. K., Gould, R. A., Gallo MacFarlane, E., Consortium, M. L. Pathophysiology of aortic aneurysm: insights from human genetics and mouse models. *Pharmacogenomics.* **17** (18), 2071-2080 (2016).
13. Adam, M. et al. Systemic Upregulation of IL-10 (Interleukin-10) Using a Nonimmunogenic Vector Reduces Growth and Rate of Dissecting Abdominal Aortic Aneurysm. *Arteriosclerosis, Thrombosis, and Vascular Biology.* **38** (8), 1796-1805 (2018).

14. Barisione, C. et al. Rapid dilation of the abdominal aorta during infusion of angiotensin II detected by noninvasive high-frequency ultrasonography. *Journal of Vascular Surgery.* **44** (2), 372-376 (2006).
15. Trachet, B. et al. Ascending Aortic Aneurysm in Angiotensin II-Infused Mice: Formation, Progression, and the Role of Focal Dissections. *Arteriosclerosis, Thrombosis, and Vascular Biology.* **36** (4), 673-681 (2016).
16. Sawada, H. et al. Heterogeneity of aortic smooth muscle cells: A determinant for regional characteristics of thoracic aortic aneurysms? *Journal of Translational Internal Medicine.* **6** (3), 93-96 (2018).
17. Davis, F. M. et al. Smooth muscle cell deletion of low-density lipoprotein receptor-related protein 1 augments angiotensin II-induced superior mesenteric arterial and ascending aortic aneurysms. *Arteriosclerosis, Thrombosis, and Vascular Biology.* **35** (1), 155-162 (2015).
18. Angelov, S. N. et al. TGF-beta (Transforming Growth Factor-beta) Signaling Protects the Thoracic and Abdominal Aorta From Angiotensin II-Induced Pathology by Distinct Mechanisms. *Arteriosclerosis, Thrombosis, and Vascular Biology.* **37** (11), 2102-2113 (2017).
19. Daugherty, A. et al. Angiotensin II infusion promotes ascending aortic aneurysms: attenuation by CCR2 deficiency in apoE-/- mice. *Clinical Science.* **118** (11), 681-689 (2010).
20. Fava, M. et al. Role of ADAMTS-5 in Aortic Dilatation and Extracellular Matrix Remodeling. *Arteriosclerosis, Thrombosis, and Vascular Biology.* **38** (7), 1537-1548 (2018).
21. Rateri, D. L. et al. Angiotensin II induces region-specific medial disruption during evolution of ascending aortic aneurysms. *The American Journal of Pathology.* **184** (9), 2586-2595 (2014).
22. Huang, X. et al. MicroRNA-21 Knockout Exacerbates Angiotensin II-Induced Thoracic Aortic Aneurysm and Dissection in Mice With Abnormal Transforming Growth Factor-beta-SMAD3 Signaling. *Arteriosclerosis, Thrombosis, and Vascular Biology.* **38** (5), 1086-1101 (2018).
23. Galatioto, J. et al. Cell Type-Specific Contributions of the Angiotensin II Type 1a Receptor to Aorta Homeostasis and Aneurysmal Disease-Brief Report. *Arteriosclerosis, Thrombosis, and Vascular Biology.* **38** (3), 588-591 (2018).
24. Habashi, J. P. et al. Losartan, an AT1 antagonist, prevents aortic aneurysm in a mouse model of Marfan syndrome. *Science.* **312** (5770), 117-121 (2006).
25. Hibender, S. et al. Resveratrol Inhibits Aortic Root Dilatation in the Fbn1C1039G/+ Marfan Mouse Model. *Arteriosclerosis, Thrombosis, and Vascular Biology.* **36** (8), 1618-1626 (2016).
26. Hu, J. H. et al. Postnatal Deletion of the Type II Transforming Growth Factor-beta Receptor in Smooth Muscle Cells Causes Severe Aortopathy in Mice. *Arteriosclerosis, Thrombosis, and Vascular Biology.* **35** (12), 2647-2656 (2015).
27. Li, W. et al. Tgfbr2 disruption in postnatal smooth muscle impairs aortic wall homeostasis. *The Journal of Clinical Investigation.* **124** (2), 755-767 (2014).
28. Yang, P. et al. Smooth muscle cell-specific Tgfbr1 deficiency promotes aortic aneurysm formation by stimulating multiple signaling events. *Scientific Reports.* **6**, 35444 (2016).
29. Dawson, D. et al. Quantitative 3-dimensional echocardiography for accurate and rapid cardiac phenotype characterization in mice. *Circulation.* **110** (12), 1632-1637 (2004).
30. Grune, J. et al. Evaluation of a commercial multi-dimensional echocardiography technique for ventricular volumetry in small animals. *Cardiovascular Ultrasound.* **16** (1), 10 (2018).

31. Phillips, E. H., Di Achille, P., Bersi, M. R., Humphrey, J. D., Goergen, C. J. Multi-Modality Imaging Enables Detailed Hemodynamic Simulations in Dissecting Aneurysms in Mice. *IEEE Transactions on Medical Imaging.* **36** (6), 1297-1305 (2017).
32. Soepriatna, A. H., Damen, F. W., Vlachos, P. P., Goergen, C. J. Cardiac and respiratory-gated volumetric murine ultrasound. *The International Journal of Cardiovascular Imaging.* **34** (5), 713-724 (2018).
33. FUJIFILM VisualSonic Inc. *Vevo3100 - the ultimate preclinical imaging experience.* https://www.visualsonics.com/product/imaging-systems/vevo-3100 (2018).
34. Shen, M. et al. Divergent roles of matrix metalloproteinase 2 in pathogenesis of thoracic aortic aneurysm. *Arteriosclerosis, Thrombosis, and Vascular Biology.* **35** (4), 888-898 (2015).
35. Trachet, B. et al. Performance comparison of ultrasound-based methods to assess aortic diameter and stiffness in normal and aneurysmal mice. *PLoS One.* **10** (5), e0129007 (2015).
36. Wang, Y. et al. TGF-beta activity protects against inflammatory aortic aneurysm progression and complications in angiotensin II-infused mice. *The Journal of Clinical Investigation.* **120** (2), 422-432 (2010).
37. Goergen, C. J. et al. In vivo quantification of murine aortic cyclic strain, motion, and curvature: implications for abdominal aortic aneurysm growth. *Journal of Magnetic Resonance Imaging.* **32** (4), 847-858 (2010).
38. Ben-Zvi, D. et al. Local Application of Leptin Antagonist Attenuates Angiotensin II-Induced Ascending Aortic Aneurysm and Cardiac Remodeling. *Journal of the American Heart Association.* **5** (5) (2016).
39. Goergen, C. J. et al. Influences of aortic motion and curvature on vessel expansion in murine experimental aneurysms. *Arteriosclerosis, Thrombosis, and Vascular Biology.* **31** (2), 270-279 (2011).
40. Phillips, E. H. et al. Morphological and Biomechanical Differences in the Elastase and AngII apoE(-/-) Rodent Models of Abdominal Aortic Aneurysms. *BioMed Research International.* **2015**, 413189 (2015).
41. Di Lascio, N., Kusmic, C., Stea, F., Faita, F. Ultrasound-based Pulse Wave Velocity Evaluation in Mice. *Journal of Visualized Experiments.* (120), e54362 (2017).
42. Lee, L. et al. Aortic and Cardiac Structure and Function Using High-Resolution Echocardiography and Optical Coherence Tomography in a Mouse Model of Marfan Syndrome. *PLoS One.* **11** (11), e0164778 (2016).

Figure 1.

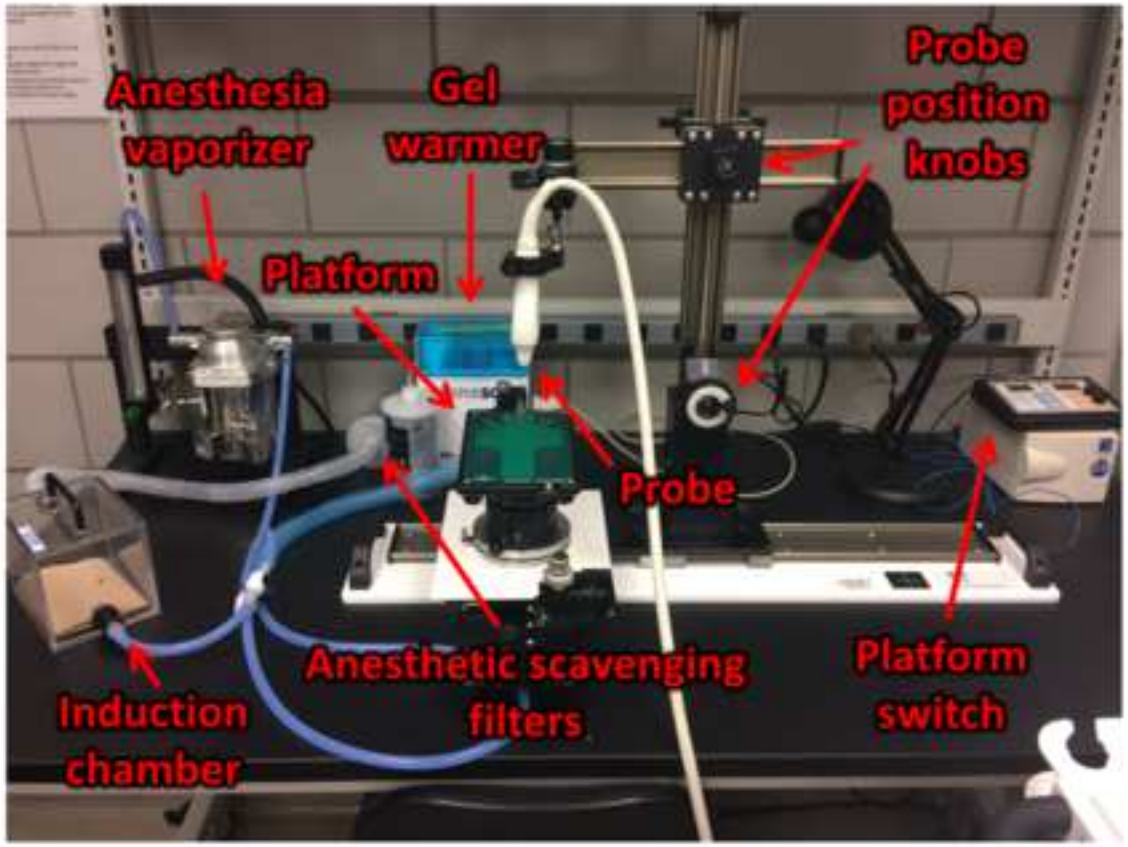

Figure 2.

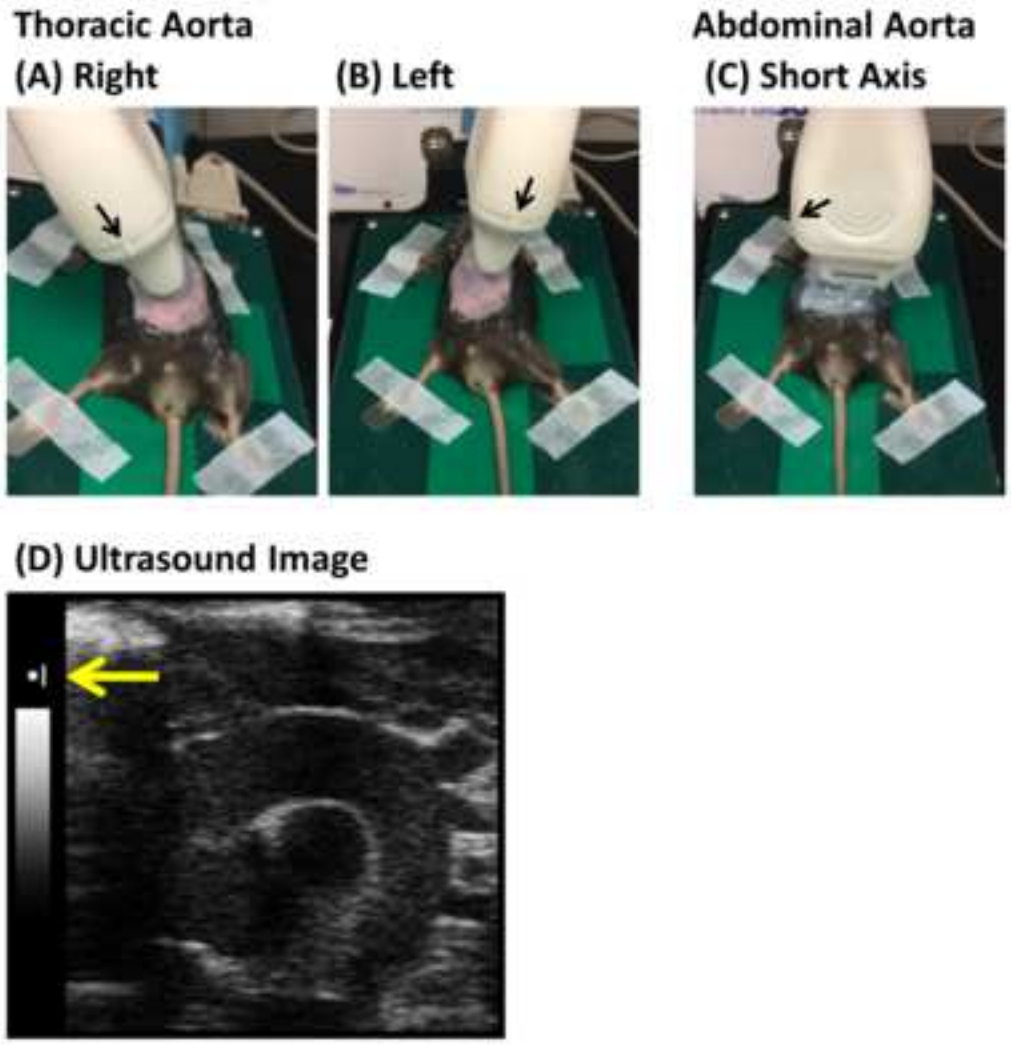

Figure 3.

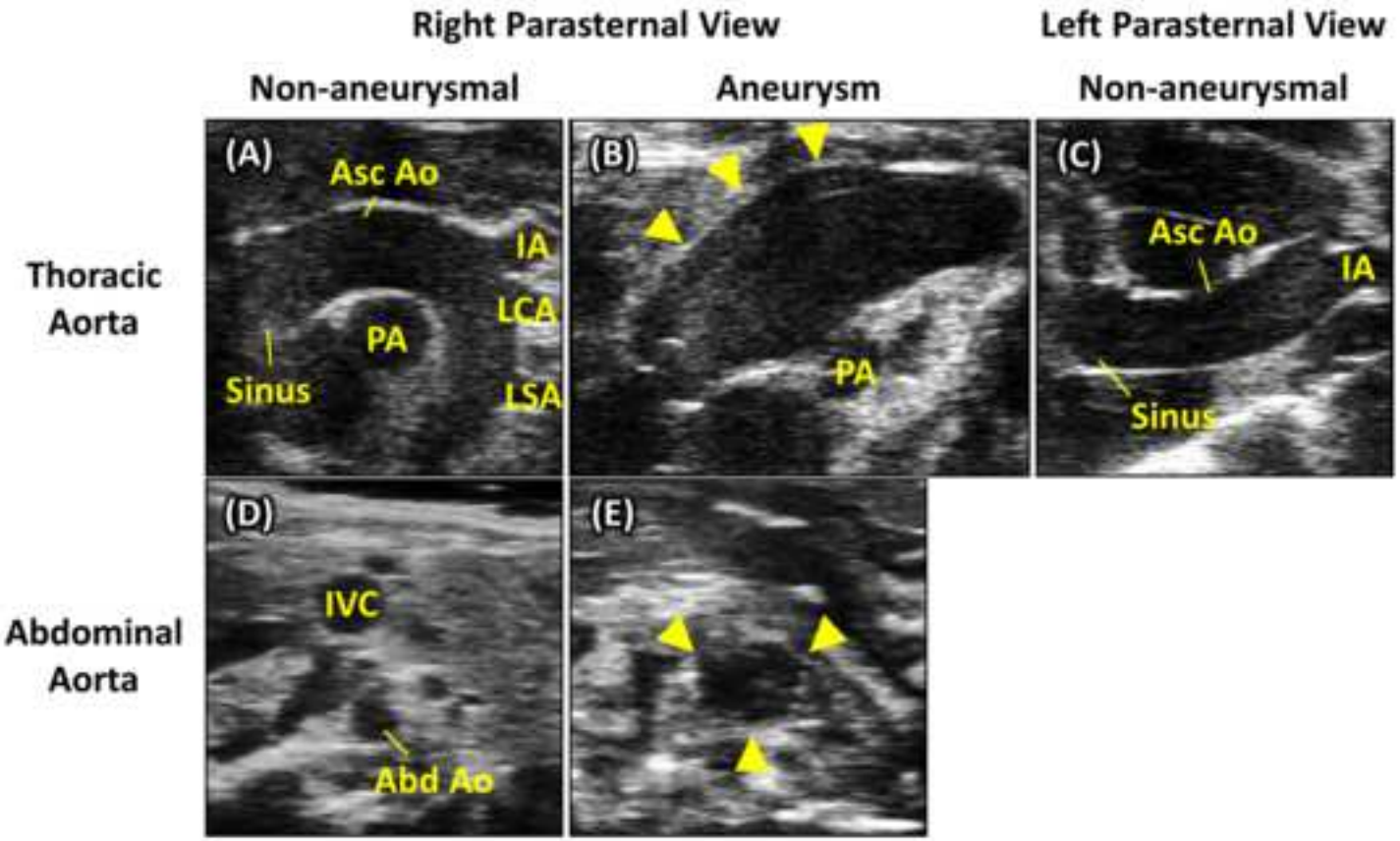

Figure 4.

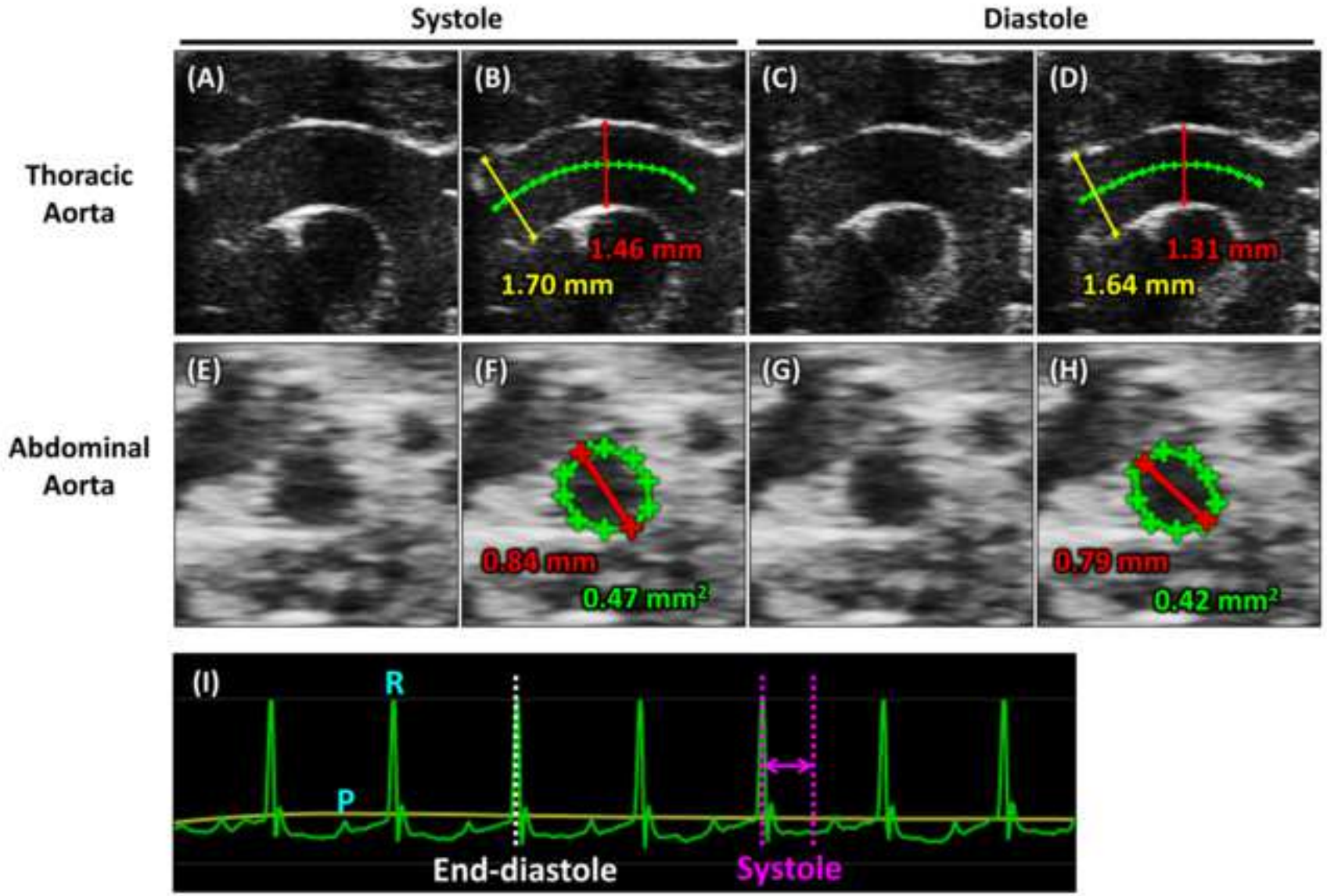

Figure 5.

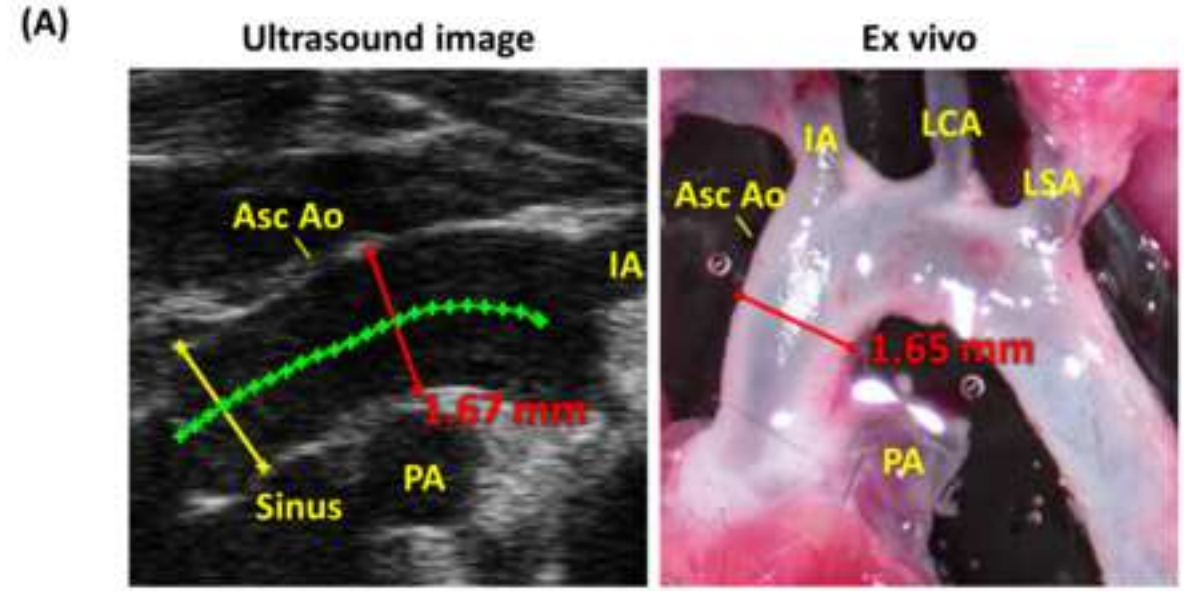

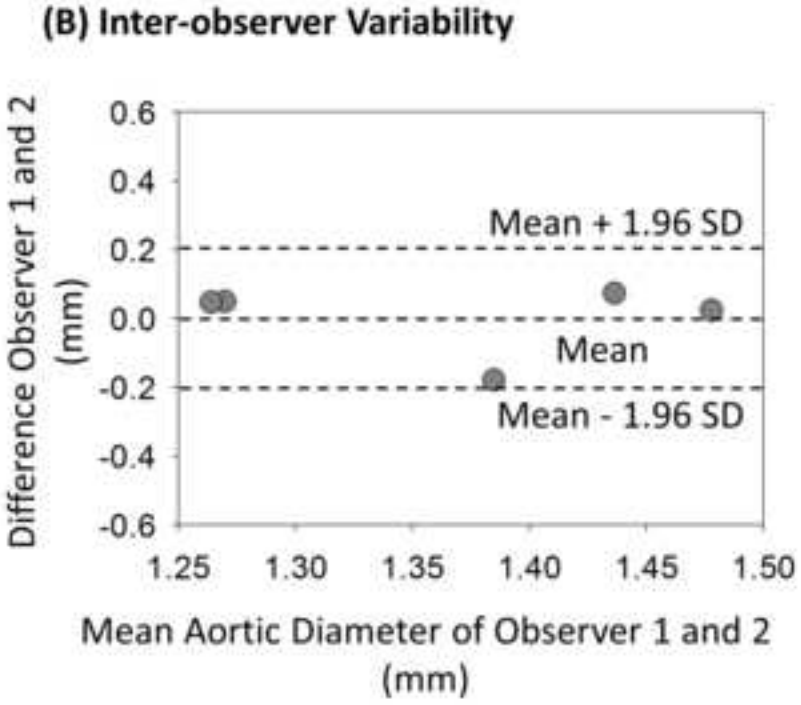

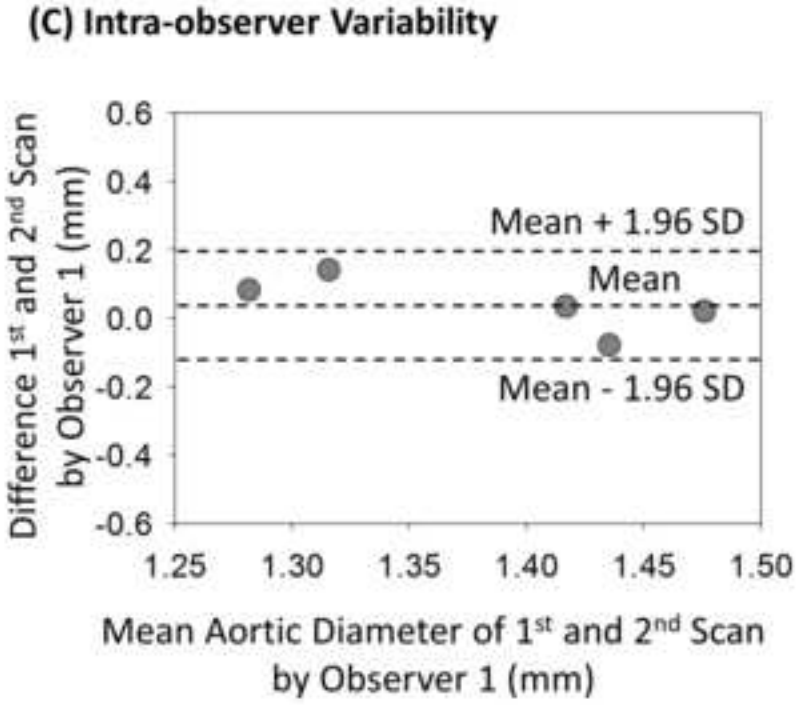

Table 1. Ultrasound settings in this protocol

Parameter	Setting
Frequency	40 MHz
Power	100%
Frame Rate	401
Gain	25.0 dB
Depth	9.00 mm
Width	7.07 mm
Capture	300 frames

Table 2. Advantages and disadvantages of the right and left parasternal long axis views

	Right	Left
Sinus	+	++
Asc Ao	++	+
Arch	++	−
Desc Ao	−	−

Right parasternal = right parasternal long axis view, Left = left parasternal long axis view,

Sinus = Aortic sinus, Asc Ao = Ascending aorta, Arch = Aortic arch, Desc Ao = Descending aorta,

++ = good visualization, + = fair visualization, − = not applicable for aortic visualization.

Table of Materials

Name of Reagent	Company	Catalog Number	Comments/Description
Isothesia (Isoflurane)	Henry Schin	NDC11695-6776-2	Anesthetic Agent
Omnicon F/Air Anesthesia Gas Filter Canister	A.M. Bickford Inc.	80120	Scavenging System for Anesthesia
Puralube Vet Ointment	Dechra	NDC17033-211-38	Lubricating Eye Drops
Aquasonic	Parker Laboratories	01-08	Ultrasound Gel
Nair	Nair		Depilliating Cream
Transeptic Transducer Cleaning Solution	Parker Laboratories	341-09-25	Cleaning spray for probes

Name of Equipment	Company	Catalog Number	Comments/Description
Vevo 2100	VisualSonics	Vevo 2100	Ultrasound Machine
Vevo LAB 3.0.0	VisualSonics	Vevo LAB 3.0.0	Ultrasound Analysis Software
MS-550D	VisualSonics	MS-550D	Ultrasound Probe
EX3 Vaporizer	Patterson Veterinary	EX 3	Analogue Anestheic Vaporizer
Heating Pad	Sunbeam	E12107	Heating Pad

jove JOURNAL OF VISUALIZED EXPERIMENTS
1 Alewife Center #200
Cambridge, MA 02140
tel. 617.945.9051
www.jove.com

ARTICLE AND VIDEO LICENSE AGREEMENT

Title of Article: Ultrasonography of the Thoracic and Abdominal Aorta in Mice to Determine Aneurysm Dimensions.

Author(s): Hisashi Sawada, Jeff Z. Chen, Bradley C. Wright, Jessica J. Moorleghen, Hong S. Lu, Alan Daugherty.

Item 1: The Author elects to have the Materials be made available (as described at http://www.jove.com/publish) via:

☐ Standard Access ☒ Open Access

Item 2: Please select one of the following items:

☒ The Author is **NOT** a United States government employee.

☐ The Author is a United States government employee and the Materials were prepared in the course of his or her duties as a United States government employee.

☐ The Author is a United States government employee but the Materials were NOT prepared in the course of his or her duties as a United States government employee.

ARTICLE AND VIDEO LICENSE AGREEMENT

1. **Defined Terms.** As used in this Article and Video License Agreement, the following terms shall have the following meanings: "**Agreement**" means this Article and Video License Agreement; "**Article**" means the article specified on the last page of this Agreement, including any associated materials such as texts, figures, tables, artwork, abstracts, or summaries contained therein; "**Author**" means the author who is a signatory to this Agreement; "**Collective Work**" means a work, such as a periodical issue, anthology or encyclopedia, in which the Materials in their entirety in unmodified form, along with a number of other contributions, constituting separate and independent works in themselves, are assembled into a collective whole; "**CRC License**" means the Creative Commons Attribution-Non Commercial-No Derivs 3.0 Unported Agreement, the terms and conditions of which can be found at: http://creativecommons.org/licenses/by-nc-nd/3.0/legalcode; "**Derivative Work**" means a work based upon the Materials or upon the Materials and other pre-existing works, such as a translation, musical arrangement, dramatization, fictionalization, motion picture version, sound recording, art reproduction, abridgment, condensation, or any other form in which the Materials may be recast, transformed, or adapted; "**Institution**" means the institution, listed on the last page of this Agreement, by which the Author was employed at the time of the creation of the Materials; "**JoVE**" means MyJove Corporation, a Massachusetts corporation and the publisher of The Journal of Visualized Experiments; "**Materials**" means the Article and / or the Video; "**Parties**" means the Author and JoVE; "**Video**" means any video(s) made by the Author, alone or in conjunction with any other parties, or by JoVE or its affiliates or agents, individually or in collaboration with the Author or any other parties, incorporating all or any portion of the Article, and in which the Author may or may not appear.

2. **Background.** The Author, who is the author of the Article, in order to ensure the dissemination and protection of the Article, desires to have the JoVE publish the Article and create and transmit videos based on the Article. In furtherance of such goals, the Parties desire to memorialize in this Agreement the respective rights of each Party in and to the Article and the Video.

3. **Grant of Rights in Article.** In consideration of JoVE agreeing to publish the Article, the Author hereby grants to JoVE, subject to **Sections 4** and **7** below, the exclusive, royalty-free, perpetual (for the full term of copyright in the Article, including any extensions thereto) license (a) to publish, reproduce, distribute, display and store the Article in all forms, formats and media whether now known or hereafter developed (including without limitation in print, digital and electronic form) throughout the world, (b) to translate the Article into other languages, create adaptations, summaries or extracts of the Article or other Derivative Works (including, without limitation, the Video) or Collective Works based on all or any portion of the Article and exercise all of the rights set forth in (a) above in such translations, adaptations, summaries, extracts, Derivative Works or Collective Works and(c) to license others to do any or all of the above. The foregoing rights may be exercised in all media and formats, whether now known or hereafter devised, and include the right to make such modifications as are technically necessary to exercise the rights in other media and formats. If the "Open Access" box has been checked in **Item 1** above, JoVE and the Author hereby grant to the public all such rights in the Article as provided in, but subject to all limitations and requirements set forth in, the CRC License.

jove JOURNAL OF VISUALIZED EXPERIMENTS
1 Alewife Center #200
Cambridge, MA 02140
tel. 617.945.9051
www.jove.com

ARTICLE AND VIDEO LICENSE AGREEMENT

4. **Retention of Rights in Article.** Notwithstanding the exclusive license granted to JoVE in **Section 3** above, the Author shall, with respect to the Article, retain the non-exclusive right to use all or part of the Article for the non-commercial purpose of giving lectures, presentations or teaching classes, and to post a copy of the Article on the Institution's website or the Author's personal website, in each case provided that a link to the Article on the JoVE website is provided and notice of JoVE's copyright in the Article is included. All non-copyright intellectual property rights in and to the Article, such as patent rights, shall remain with the Author.

5. **Grant of Rights in Video – Standard Access.** This **Section 5** applies if the "Standard Access" box has been checked in **Item 1** above or if no box has been checked in **Item 1** above. In consideration of JoVE agreeing to produce, display or otherwise assist with the Video, the Author hereby acknowledges and agrees that, Subject to **Section 7** below, JoVE is and shall be the sole and exclusive owner of all rights of any nature, including, without limitation, all copyrights, in and to the Video. To the extent that, by law, the Author is deemed, now or at any time in the future, to have any rights of any nature in or to the Video, the Author hereby disclaims all such rights and transfers all such rights to JoVE.

6. **Grant of Rights in Video – Open Access.** This **Section 6** applies only if the "Open Access" box has been checked in **Item 1** above. In consideration of JoVE agreeing to produce, display or otherwise assist with the Video, the Author hereby grants to JoVE, subject to **Section 7** below, the exclusive, royalty-free, perpetual (for the full term of copyright in the Article, including any extensions thereto) license (a) to publish, reproduce, distribute, display and store the Video in all forms, formats and media whether now known or hereafter developed (including without limitation in print, digital and electronic form) throughout the world, (b) to translate the Video into other languages, create adaptations, summaries or extracts of the Video or other Derivative Works or Collective Works based on all or any portion of the Video and exercise all of the rights set forth in (a) above in such translations, adaptations, summaries, extracts, Derivative Works or Collective Works and (c) to license others to do any or all of the above. The foregoing rights may be exercised in all media and formats, whether now known or hereafter devised, and include the right to make such modifications as are technically necessary to exercise the rights in other media and formats. For any Video to which this **Section 6** is applicable, JoVE and the Author hereby grant to the public all such rights in the Video as provided in, but subject to all limitations and requirements set forth in, the CRC License.

7. **Government Employees.** If the Author is a United States government employee and the Article was prepared in the course of his or her duties as a United States government employee, as indicated in **Item 2** above, and any of the licenses or grants granted by the Author hereunder exceed the scope of the 17 U.S.C. 403, then the rights granted hereunder shall be limited to the maximum rights permitted under such statute. In such case, all provisions contained herein that are not in conflict with such statute shall remain in full force and effect, and all provisions contained herein that do so conflict shall be deemed to be amended so as to provide to JoVE the maximum rights permissible within such statute.

8. **Protection of the Work.** The Author(s) authorize JoVE to take steps in the Author(s) name and on their behalf if JoVE believes some third party could be infringing or might infringe the copyright of either the Author's Article and/or Video.

9. **Likeness, Privacy, Personality.** The Author hereby grants JoVE the right to use the Author's name, voice, likeness, picture, photograph, image, biography and performance in any way, commercial or otherwise, in connection with the Materials and the sale, promotion and distribution thereof. The Author hereby waives any and all rights he or she may have, relating to his or her appearance in the Video or otherwise relating to the Materials, under all applicable privacy, likeness, personality or similar laws.

10. **Author Warranties.** The Author represents and warrants that the Article is original, that it has not been published, that the copyright interest is owned by the Author (or, if more than one author is listed at the beginning of this Agreement, by such authors collectively) and has not been assigned, licensed, or otherwise transferred to any other party. The Author represents and warrants that the author(s) listed at the top of this Agreement are the only authors of the Materials. If more than one author is listed at the top of this Agreement and if any such author has not entered into a separate Article and Video License Agreement with JoVE relating to the Materials, the Author represents and warrants that the Author has been authorized by each of the other such authors to execute this Agreement on his or her behalf and to bind him or her with respect to the terms of this Agreement as if each of them had been a party hereto as an Author. The Author warrants that the use, reproduction, distribution, public or private performance or display, and/or modification of all or any portion of the Materials does not and will not violate, infringe and/or misappropriate the patent, trademark, intellectual property or other rights of any third party. The Author represents and warrants that it has and will continue to comply with all government, institutional and other regulations, including, without limitation all institutional, laboratory, hospital, ethical, human and animal treatment, privacy, and all other rules, regulations, laws, procedures or guidelines, applicable to the Materials, and that all research involving human and animal subjects has been approved by the Author's relevant institutional review board.

11. **JoVE Discretion.** If the Author requests the assistance of JoVE in producing the Video in the Author's facility, the Author shall ensure that the presence of JoVE employees, agents or independent contractors is in accordance with the relevant regulations of the Author's institution. If more than one author is listed at the beginning of this Agreement, JoVE may, in its sole

jove JOURNAL OF VISUALIZED EXPERIMENTS
1 Alewife Center #200
Cambridge, MA 02140
tel. 617.945.9051
www.jove.com

ARTICLE AND VIDEO LICENSE AGREEMENT

discretion, elect not take any action with respect to the Article until such time as it has received complete, executed Article and Video License Agreements from each such author. JoVE reserves the right, in its absolute and sole discretion and without giving any reason therefore, to accept or decline any work submitted to JoVE. JoVE and its employees, agents and independent contractors shall have full, unfettered access to the facilities of the Author or of the Author's institution as necessary to make the Video, whether actually published or not. JoVE has sole discretion as to the method of making and publishing the Materials, including, without limitation, to all decisions regarding editing, lighting, filming, timing of publication, if any, length, quality, content and the like.

12. **Indemnification.** The Author agrees to indemnify JoVE and/or its successors and assigns from and against any and all claims, costs, and expenses, including attorney's fees, arising out of any breach of any warranty or other representations contained herein. The Author further agrees to indemnify and hold harmless JoVE from and against any and all claims, costs, and expenses, including attorney's fees, resulting from the breach by the Author of any representation or warranty contained herein or from allegations or instances of violation of intellectual property rights, damage to the Author's or the Author's institution's facilities, fraud, libel, defamation, research, equipment, experiments, property damage, personal injury, violations of institutional, laboratory, hospital, ethical, human and animal treatment, privacy or other rules, regulations, laws, procedures or guidelines, liabilities and other losses or damages related in any way to the submission of work to JoVE, making of videos by JoVE, or publication in JoVE or elsewhere by JoVE. The Author shall be responsible for, and shall hold JoVE harmless from, damages caused by lack of sterilization, lack of cleanliness or by contamination due to the making of a video by JoVE its employees, agents or independent contractors. All sterilization, cleanliness or decontamination procedures shall be solely the responsibility of the Author and shall be undertaken at the Author's expense. All indemnifications provided herein shall include JoVE's attorney's fees and costs related to said losses or damages. Such indemnification and holding harmless shall include such losses or damages incurred by, or in connection with, acts or omissions of JoVE, its employees, agents or independent contractors.

13. **Fees.** To cover the cost incurred for publication, JoVE must receive payment before production and publication of the Materials. Payment is due in 21 days of invoice. Should the Materials not be published due to an editorial or production decision, these funds will be returned to the Author. Withdrawal by the Author of any submitted Materials after final peer review approval will result in a US$1,200 fee to cover pre-production expenses incurred by JoVE. If payment is not received by the completion of filming, production and publication of the Materials will be suspended until payment is received.

14. **Transfer, Governing Law.** This Agreement may be assigned by JoVE and shall inure to the benefits of any of JoVE's successors and assignees. This Agreement shall be governed and construed by the internal laws of the Commonwealth of Massachusetts without giving effect to any conflict of law provision thereunder. This Agreement may be executed in counterparts, each of which shall be deemed an original, but all of which together shall be deemed to me one and the same agreement. A signed copy of this Agreement delivered by facsimile, e-mail or other means of electronic transmission shall be deemed to have the same legal effect as delivery of an original signed copy of this Agreement.

A signed copy of this document must be sent with all new submissions. Only one Agreement is required per submission.

CORRESPONDING AUTHOR

Name:	Alan Daugherty
Department:	Saha CVRC
Institution:	University of Kentucky
Title:	Professor
Signature:	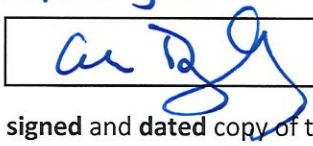
Date:	8/29/2018

Please submit a **signed** and **dated** copy of this license by one of the following three methods:

1. Upload an electronic version on the JoVE submission site
2. Fax the document to +1.866.381.2236
3. Mail the document to JoVE / Attn: JoVE Editorial / 1 Alewife Center #200 / Cambridge, MA 02140

Response to Reviewers' Comments: JoVE59013

Title: Ultrasound Imaging of the Thoracic and Abdominal Aorta in Mice to Determine Aneurysm Dimensions

We thank the Editor and Reviewers for their constructive comments and suggestions to improve this manuscript. The Editor's and Reviewers' comments are in **bold** followed by our responses point by point. Changes in the revised manuscript are distinguished in red color.

We hope that this version has successfully incorporated the Editor's and Reviewers' points, and the scientific quality has been improved substantially.

Response to the Editor:

1. Please take this opportunity to thoroughly proofread the manuscript to ensure that there are no spelling or grammar issues.

Authors' reply:

We have carefully checked spelling and grammar.

2. Please do not highlight notes for filming.

Authors' reply:

This has been corrected.

3. Please use h, min, s for time units.

Authors' reply:

All time units have been revised as requested.

4. For steps that are done using software, a step-wise description of software usage must be included in the step. Please mention what button is clicked on in the software, or which menu items need to be selected to perform the step.

Authors' reply:

We have revised Section 6 to provide the detailed steps of measuring aortic dimensions using the Vevo 2100 system. Example image of the computer screen is shown in Supplemental Figure 1.

5. Please do not abbreviate journal titles for all references.

Authors' reply:

Journal titles in the references section have been revised as requested.

6. Please upload each Figure individually to your Editorial Manager account as a .png or a .tiff file.

Authors' reply:

All figures have been uploaded individually as a PNG file.

Response to the Editor:

1. Please take this opportunity to thoroughly proofread the manuscript to ensure that there are no spelling or grammar issues.

Authors' reply:

Thank you for your comments. We have corrected all spelling and grammar issues.

2. 2.1: Please specify the age, gender and strain of mouse. Please indicate the concentration of isoflurane.

Authors' reply:

Ten to twelve week-old C57BL/6J male mice (n = 5) were used for the experiments in this study. We have included this information in the figure legends.

We used 1.5 – 2.5 % vol/vol isoflurane with 1 L/min oxygen. We have revised (1.6) and (2.2) to include the concentrations of isoflurane and oxygen.

3. 2.2: Please mention how to confirm that mouse is anesthetized.

Authors' reply:

Loss of withdrawal reflex was used as the index to confirm the depth of anesthesia. We have added this information to (2.3).

4. 2.6: Providing an estimate for the delivery rate of anesthesia may be helpful.

Authors' reply:

We used 1.5 – 2.5 % vol/vol isoflurane with 1 L/min oxygen. We have revised (1.6) and (2.2) to describe the concentrations of isoflurane and oxygen.

5. 3.4 and 3.5: Are these done by using the instrument software? Please specify.

Authors' reply:

Images were cropped using a standard tool in the Vevo 2100 ultrasound system during ultrasound imaging. We have revised (3.5) and (3.6).

6. Lines 169-178; Please include these details in a separate step and write them in imperative tense if possible. Any text that cannot be written in the imperative tense should be added as a "Note".

Authors' reply:

This paragraph has been moved to the "Note" of (3.4).

7. Line 196: Please avoid the use of any personal pronouns.

Authors' reply:

Personal pronouns have been replaced.

8. Please ensure that the highlighted part of the step includes at least one action that is written in imperative tense. Please do not highlight any steps describing anesthetization and euthanasia.

Authors' reply:

The text has been modified in accord with these suggestions.

9. Discussion: Please discuss critical steps within the protocol and any limitations of the technique.

Authors' reply:

Critical steps and limitation has been included in a paragraph in the discussion.

10. For in-text references, the corresponding reference numbers should appear as superscripts after the appropriate statement(s) in the text (before punctuation but after closed parenthesis).

Authors' reply:

The corresponding reference numbers have been revised as requested.

11. References: If there are six or more authors, list the first author and then "et al.". Please do not abbreviate journal titles.

Authors' reply:

The author lists have been corrected.

Response to Reviewer #1:

Major Concerns:

1) Preparation of Mouse (section 2.1) - "Place the mouse in isoflurane/O2-filled induction chamber." It is actually recommended in codes of practice that the mouse is placed in the induction chamber before filling with isoflurane as this reduces stress experienced by the mouse and avoids any unwanted cardiovascular effects from anaesthetic shock that may affect the experiment. The induction chamber should ideally be pre-filled with oxygen and then gradually filled with anaesthetic once the mouse is in the chamber. This is particularly important when running longitudinal studies.

Authors' reply:

We appreciate this important suggestion. Section (1.6) – (2.2) have been edited to include this suggestion. As suggested by the Reviewer #1, to minimize unwanted cardiovascular changes due to anesthesia, experimental mice should be placed in an O_2-filled chamber and then anesthesia should be filled gradually in the chamber.

2) Analysis of abdominal aortic images (section 6.2.2) - I would say it is essential to measure at a consistent phase of the cardiac cycle, even in the abdominal aorta, as not to do so would introduce an unwanted (and unnecessary) extra layer of variability in the analysis. A recent ultrasound study of mouse abdominal aorta actually quantified % distension from the change in aortic diameter over the cardiac cycle. In a naïve, WT mouse this can be as high as 20% on average. This point is actually made later on in the Discussion, therefore the ambiguity in 6.2.2 should be removed.

Authors' reply:

Thank you very much for your comments. For accurate measurements in both the thoracic and abdominal aortas, the cardiac cycle should be taken into consideration. Section (6.2.2) has been revised to remove the ambiguity.

Minor Concerns:

1) Preparation of Mouse (section 2) - there is no mention of use of an anaesthetic scavenging system in the text, although it is evident in Figure 1. Also, was temperature monitored during imaging (e.g. using rectal thermometer probe)?

Authors' reply:

Information on the scavenging system has been included in (1.4) and Figure 1. In this protocol, mouse was placed on the heated platform at 37.0 °C, but temperature was not monitored using a rectal thermometer probe.

2) Imaging of thoracic aorta (section 3) - it would be a good idea to list typical ultrasound

parameters used (e.g. frame rate, depth, gain, etc), possibly in a table, to assist an inexperienced ultrasound operator.

Authors' reply:

The usual ultrasound parameters are now included in the table (3.7).

3) Imaging of the abdominal aorta (section 4.2) - suggest including pulsed wave Doppler in the imaging protocol to confirm pulsatile blood flow. Without this step, vena cava / portal vein may be mistaken for the abdominal aorta by an inexperienced operator, particularly in an aneurysm model where the artery is enlarged.

Authors' reply:

As the Reviewer #1 suggested, pulse wave Doppler is useful method to measure the blood velocity. However, it is often difficult to detect the blood flow accurately in the abdominal aorta, because the axis of the abdominal aorta is not parallel to echo beam in this method. Thus, the abdominal aorta was distinguished from the vena cava and portal vein by color Doppler and pressing down on the probe. The vena cava and portal vein are compressible, while the aorta maintains its patency. We have added this step into (4.2).

4) Analysis of thoracic aortic images (section 6.1.2) - which phase of the cardiac cycle do you typically use for analysis? This relates to Major Concern no. 2. The cardiac phase used should be stated clearly in the protocol. Also, more detail could be provided on how the measurements were performed in the abdominal aorta. Assuming image acquisition is reproducible, the analysis method is the key to reliability and reproducibility of the method as a whole. The authors should state whether the measurement was inner edge to inner edge of the vessel lumen (as stated for thoracic aorta measurements), outer to outer, etc.

Authors' reply:

We routinely measure aortic diameters at the end of diastole, partially based on the ease of defining this phase in the ECG. We have added these comments into (6.1.2).

As with thoracic measurements, abdominal aortic diameter is measured from the inner edge to inner edge of the vessel lumen. This suggestion is now included in (6.2.2) and (6.2.4).

Response to Reviewer #2:

Major Concerns:

1. No mention is made regarding the infrarenal aorta. While many mouse models of AAAs are suprarenal, infrarenal models obviously do exist. Further, the vast majority of human abdominal aortic aneurysms occur in the infrarenal portion. The authors may want to consider including a section on imaging the infrarenal aorta and the best strategies for this region (i.e. changing the table orientation if abdominal gas creates an artifact).

Authors' reply:

This protocol can also be used to measure the diameter of the infra-renal aorta. We have revised Section 4 to reflect this ability.

2. Line 355: As AAAs enlarge, they too can become tortuous. Keeping the same probe position for all images may result in artificially larger measurements as they could be taken off axis. Recommend mention of staying along the true transverse axis of the vessel.

Authors' reply:

The text of the note is (4.6) has been amended to include "adjustment of the probe angle is needed for accurate aortic imaging".

3. Line 357: The discussion fails to mention recent advancements in 3D and 4D vascular ultrasound. Recommend adding this to the discussion as many of the issues associated with M-mode and B-mode are alleviated with these volumetric approaches (PMIDs: 15364813, 10511652, 29234935, 29234935, 29966517).

Authors' reply:

The advantages of 3D and 4D imaging have been included in the discussion section.

4. Line 371: The discussion on vessel "elasticity" is lacking. Ultrasound images can be used to measure vessel distention or strain. Calculations of vessel elasticity, stiffness, or pressure-strain elastic modulus require measurements and assumptions related to vessel loading (i.e. systolic, diastolic, and pulse pressures). Aneurysms certainly lead to stiffer vessels due to elastin breakdown and increased collagen deposition (PMID: 21071686, 26064906, 28186882), but ultrasound cannot measure vessel stiffness directly. Recommend rewording and expanding this section to clarify for the reader.

Authors' reply:

The discussion has been revised and expanded to explain aortic elasticity, strain, and stiffness.

Minor Concerns:

1. No mention is made of a method to determine depth of anesthesia. I would suggest mention of the withdrawal reflex.

Authors' reply:

In accord with the reviewer's suggestions, "monitoring the withdrawal reflex" has been added to (2.3).

2. No mention is made of adjusting overall gain or time gain compensation. Most ultrasound systems now are user friendly and need very little tweaking, but these (especially overall gain) seem too important to leave out.

Authors' reply:

As the Reviewer #2 mentioned, ultrasound settings are important to image tissues accurately. A table (Table 1) has been included to describe the ultrasound setting including overall gain in (3.7).

3. Throughout the paper the authors instruct the reader to do something in a specific direction. The authors use both the mouse's orientation and the reader's orientation. For example, lines 170-177 reference the mouse's left parasternal area, but in line 184 the reader is instructed that the "notch" should be on the left. Is this the mouse's left? Or the reader's left? To avoid confusion, I would recommend being clear and sticking with either the mouse's orientation or self-orientation, not both.

Authors' reply:

We apologize for these ambiguous instructions. The text has been modified (4.1) to the mouse's orientation.

4. Line 127: The authors instruct the reader to apply depilatory cream to the chest and abdomen. Most studies will only be looking at one area. As depilatory cream removes hair using chemicals, thoughtful restraint to be careful not to scar the mouse's skin and limit the area in which it is applied is recommended.

Authors' reply:

In accord with the reviewers suggestions "Use of depilatory creams should be kept to the minimum to avoid irritation" has been added to (2.7).

5. Line 135: 400-500 bpm seems slow. Our mice typically have anesthetized heart rates above 500 unless they are hypothermic. Recommend adjusting this range.

Authors' reply:

We apologize for this mistake. Mice show typically around 500 bpm of HR during anesthesia. However, some mice with aneurysms have slightly lower heart rate than control mice during the procedure, even when on a heated platform and anesthetized using an

appropriate dose of isoflurane. We have revised appropriate heart rate range to 450 – 550 bpm.

6. Line 148: New users may not understand what the "notch" is, especially since it varies between ultrasound systems. A picture or brief explanation could demystify this.

Authors' reply:

We acknowledge that the "notch" was not an appropriate word for new users. The "reference marker" has been revised and added black arrows to indicate the marker in Figure 2A-D, and provided a brief explanation of the reference marker in the text (3.2).

7. Line160: Cropping the ultrasound image does not improve spatial resolution. Lateral resolution changes only with focal depth and axial resolution is dependent on spatial pulse length, which can only be improved with higher frequency.

Authors' reply:

We apologize for this mistake. Images are cropped to increase the frame rate. This error has been corrected.

8. Figure 2B/Line 171: In this figure the stage looks like it has been tilted back to level again. Previously the stage was tilted to the mouse's left. Is the stage still tilted?

Authors' reply:

For the right parasternal long axis view, the stage tilts to the mouse's left. Conversely, in the left parasternal long axis view, the stage is flat or tilts to the mouse's right slightly. This information has been added in (3.4).

9. Line 185: Color Doppler signal may occasionally fail to appear in the vessel if the Doppler angle is at 90 degrees. Recommend briefly mentioning Doppler steering parallel to the vessel.

Authors' reply:

The reviewer's suggestion has been incorporated in (4.2).

10. Line 199: This needs clarification: do the authors recommend taking one cine loop from the SMA all the way down to the renal arteries? Or is one cine loop simply capturing several heart beats at one specific location? If so, what location is recommended?

Authors' reply:

We apologize for the insufficient explanation. One cine loop is captured at one specific location showing the maximum expansion in region of interest of the abdominal aorta. The imaging location is described in (4.7).

11. Line 211: Ultrasound machines are expensive and very sensitive to chemicals. I would suggest the authors include a line recommending the reader check with the ultrasound

vendor to determine what chemicals are acceptable for cleaning the ultrasound system.

Authors' reply:

Cleaning of the transducer has been included in (5.4) after consultation with FUJIFILM VisualSonics, Inc.. After every imaging session, the probe should be wiped gently with a soft cloth and isopropyl alcohol or glutaraldehyde wipes.

12. Scant grammatical errors, such as line 245: In the context the authors are using it, mean is not a verb. Suggest replacement with the word average; Line 234: remove the word "and"; Line 173: insert the word "an" between the words "acquire" and "aortic".

Authors' reply:

Grammatical issues have been corrected.

13. Line 333: Avoid stating there are "modes" of probe placement. For the average imaging researcher, the word modes refers to B-mode, M-mode, etc.

Authors' reply:

In accord with the reviewer's suggestion, "modes" has been replaced with "approach".

14. Figure 4: One other option when estimating diameter from short axis views is to calculate an "effective diameter" based on the Area of the vessel and the assumption of a circular cross-section (A = Pi/4*D^2). This is likely a better way than simply drawing a linear measurement at one orientation.

Authors' reply:

The aorta is cylindrical, but its cross section is not a perfect circle. In this protocol, the maximum diameter was measured. Thus, the assumption of a circular cross-section based on this measurement has a potential to cause over estimation of aortic diameter. In this protocol, actual area was obtained by drawing the inner edge of the aorta, instead of a calculated aortic area.

Response to Reviewer #3:

Major Concerns:

Although current manuscript concisely describes how to obtain the data, the reproducibility of the data has not been demonstrated in the current manuscript. Addition of several points would further strengthen the current manuscript.

Authors' reply:

Thank you for your constructive suggestion. This revision includes figures showing the reproducibility of this protocol. To examine the reproducibility, ultrasonography was performed on two different days using the same mice by two different investigators; an experienced cardiologist and a non-experienced student. Aortic diameter measurements between these two operators were in close agreement (Figure 5B, C).

Minor Concerns:

1. The authors mentioned "confounding factors" and "confounders" in the manuscript without defining them. Please define these factors.

Authors' reply:

Probe position and cardiac cycle have an impact to cause measurement errors as confounders. These factor are now included in the abstract and discussion.

2. It would be important to demonstrate the reproducibility of the data that were obtained by the provided method. Please provide the intra-observer and inter-observer variabilities of the data.

Authors' reply:

Figures have been added to demonstrate the intra- and inter-observer variabilities of this protocol in Figure 5B and C. There was no major variability of intra- and inter-observers. These data have been included in the representative results section.

3. Please state anatomical landmark(s), if available, for the thoracic aorta to judge whether the obtained images are appropriate for the reproducible morphometry in a single animal and among different animals.

Authors' reply:

The aortic valve and innominate and pulmonary arteries were used as anatomical landmarks, as now stated in (3.4).

4. Two approaches are recommended for the measurement of the thoracic aorta; right and left parasternal approaches. Providing the representative images for each approach would be helpful. Also, please summarize the advantages and disadvantages of each approach in a

concise manner.

Authors' reply:

Section (3.4) has been revised and a table (Table 2) added to describe the advantages and disadvantages of right and left parasternal long axis views.

5. Please state how "mid-systole" is defined.

Authors' reply:

The term 'mid-systole" is defined as the cardiac phase when the aorta is maximally expanded. Section (6.1.2) has been revised to define the mid-systole.

6. The term "dilated" should be consistently used for diseased aorta, not for the expansion of aorta due to the physiological beating.

Authors' reply:

To avoid confusion, "dilated" has replaced "expanded".

7. What are "Pre" and "Post" in Figure 4?

Authors' reply:

We apologize for this confusing mistake. "Pre" and "Post" have been deleted from the Figure 4.

Response to Reviewer #4:

Major Concerns:

Despite the fact that the authors have decided to focus only on aortic diameter measurements in mice; it is important to note the majority of recent publications in the field include measurements of Pulse Wave Velocity (PWV) as a proxy for aortic wall stiffness in mice, which has significant values in animal studies, and can be compared with with elasticity index measured in human aneurysm patients. For this reason, I think this manuscript will be significantly improved and become more of interest to the wide audience if the author includes a section on methods for PWV measurements in mice. In addition, I would like to suggest that the authors use the phrase "Ultrasound Imaging" instead of "Ultrasonography", as the former seems to be more common in current literature.

Authors' reply:

We appreciate your constructive comments. Measurements of PWV have been added in the discussion section. The manuscript has been edit to state "ultrasound imaging" instead of "ultrasonography".

Minor Concerns:

*** Line 85; replace "cylindrical shape" with "cylindrical organ"**

Authors' reply:

This has been corrected.

*** Line 90; replace "high resolution" with "high-resolution"**

Authors' reply:

This has been corrected.

*** Line 97; replace "… for mice is performed" with "… for mice was performed"**

Authors' reply:

This has been corrected.

*** Line 101; replace "Eye ointment" with "Eye lubricant"**

Authors' reply:

This has been corrected.

*** Section 3.1; replace "to the left of mouse" with " to the left side of the mouse"**

Authors' reply:

This has been corrected.

*** Section 3.3; Would the use of color Doppler help with finding the best position at this stage?**

Authors' reply:

The use of color Doppler has been included in section (3.3).

*** Section 3.3; under the "Note" section explain what are the situations in which the entire ascending aorta cannot be captured in one scan? If the image is captured separately, what are the limitation with respect to data analysis?**

Authors' reply:

Aortic pathologies such as aortic dilation and tortuosity could cause this difficulty and measurement errors. Section (3.4) has been revised.

*** Section 6.1.2; How do you select your images? how many images do you capture for each mouse? How many systole/diastole cycles would you include in your image analysis. Please create a section explaining your image selection for analysis.**

Authors' reply:

In this protocol, we used 401 frame rates and the mouse heart rate was around 500 beat per minute. Ultrasound images were captured for 300 frames. Therefore, 6 to 7 beats can be technically detected in one cine loop. Three images are selected for measurements from each cardiac cycle in the cine loop. The revised manuscript describes image selection (6.1.2, 6.1.5).

*** Section 6.1.3; How do you determine the center of the lumen? How do you make sure that you are consistent between your samples while drawing the central line?**

Authors' reply:

Since the center line was only used for the guide of drawing measurement lines of aortic dimension, the center line was drawn based on visual inspection.

*** Sections 6.1.5 and 6.2.5; are measurements for three cycles (hear beat) enough? There are publications in which they suggest using at least 5 cycles.**

Authors' reply:

There was no major deviation in our data of inner- and intra-observer variabilities for aortic measurements. Therefore, we consider three cardiac cycles are sufficient accurate measurements of aortic dimension.

*** Line 276; Please clarify for the readers why you decide to capture the aortic images at mid-systole and not end-systole.**

Authors' reply:

In mice, it is technically difficult to define the end-systole. In addition, the aorta should be maximally expanded in the mid-systole, but not in the end-systole. Therefore, aortic images were captured at the mid-systole. The text has been revised to provide the rationale for measurement at the mid-systole.

*** Clarify in your figure legends and text that the yellow line shows respiratory cycle vs. green for ECG.**

Authors' reply:

Explanations of yellow and green lines have been added to the figure legend.

Supplemental Figure 1.